IEEE Photonics Journal
An IEEE Photonics Society Publication

Open Access

Cross-Polarized Dual-Frequency VECSEL at 1.5 μm for Fiber-Based Sensing Applications

Volume 8, Number 6, December 2016

Lea Chaccour
Guy Aubin
Kamel Merghem
Jean-Louis Oudar
Aghiad Khadour
Patrice Chatellier
Sophie Bouchoule

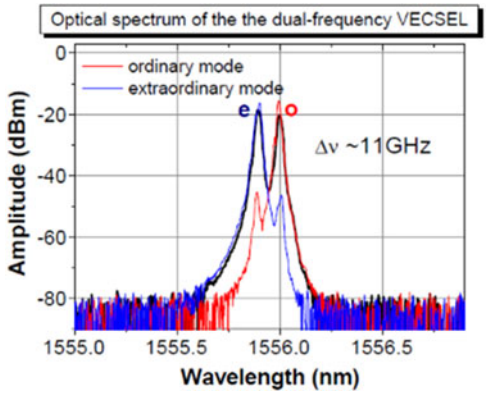

DOI: 10.1109/JPHOT.2016.2619058
1943-0655

IEEE photonics SOCIETY

IEEE

Cross-Polarized Dual-Frequency VECSEL at 1.5 μm for Fiber-Based Sensing Applications

Lea Chaccour,[1,2] Guy Aubin,[2] Kamel Merghem,[2] Jean-Louis Oudar,[2] Aghiad Khadour,[1] Patrice Chatellier,[1] and Sophie Bouchoule[2]

[1]French Institute of Science and Technology for Transport, Development and Networks, Laboratoire Interdisciplinaire Sciences Innovations Sociétés, Marne-la-Vallée 77454, France
[2]Laboratoire de Photonique et de Nanostructures, Centre National de la Recherche Scientifique UPR20, Route de Nozay 91460, France

DOI:10.1109/JPHOT.2016.2619058

Manuscript received September 28, 2016; accepted October 14, 2016. Date of publication October 21, 2016; date of current version November 7, 2016. This work was supported in part by the French Institute of Science and Technology for Transport, Development, and Networks, France, and in part by the Centre National de la Recherche Scientifique, France. Corresponding author: L. Chaccour (e-mail: lea.chaccour@ifsttar.fr).

Abstract: We have realized a dual-frequency vertical external cavity surface emitting laser (VECSEL) at 1.5 μm. Laser emission of two orthogonally polarized cavity modes is obtained by inserting a birefringent crystal into the VECSEL cavity. We have examined the influence of the different intracavity elements on the laser emission. It is shown that optimizing the free spectral range and the bandwidth of the intracavity Fabry–Perot etalon is of practical importance to achieve a stable single longitudinal laser emission for each of the two orthogonal polarizations. The optimization of the output power has also been investigated, and it is concluded that up to 50 mW output power can be expected in dual-frequency operation by adjusting the reflectivity of the output coupling mirror of the VECSEL cavity. The influence of different parameters on the stability of the dual-frequency emission has been studied. It is concluded that mechanical vibrations are the main cause of radio-frequency (RF) signal instability in our free-running VECSEL cavity. The design of a compact or mono-block cavity may allow meeting the stability requirements for optical fiber sensors based on Brillouin scattering.

Index Terms: Semiconductor lasers, diode-pumped lasers, dual-frequency lasers, Brillouin scattering, optical fiber sensors.

1. Introduction

One existing dual-frequency laser technology is based on the insertion of a birefringent element in a laser cavity. This causes the cavity with only one geometric length to become a cavity with two different effective optical lengths for the two orthogonally polarized modes. As a result, the longitudinal laser mode is split into two frequency-shifted, longitudinal modes [1]–[5]. Dual-frequency laser technology has been intensively studied for decades for application to the measurement of velocity, displacement, and acceleration [6]–[8]. Another important domain of application of dual frequency lasers is the generation and processing of optically carried radio-frequency (RF) signals [9]–[12]. The generation of RF signals using dual frequency lasers is an alternative solution to modulation techniques allowing to generate optically-carried high-frequency microwave signals

with a high spectral purity but requiring several high-frequency electronic and optical components [13], [14]. Optical heterodyning using two lasers is another solution for the generation of single-side-band signals, using more simple systems. However, a high-performance phase-locked loop is necessary in this case to maintain the spectral purity of the beat-note [15]–[17].

Dual frequency lasers could also be applied to distributed optical fiber sensors (OFS) based on Brillouin scattering, aiming at operating such systems in a low-frequency range [18]. Indeed, if the generated frequency difference is close to the Brillouin frequency v_B ($v_B \sim 11$ GHz for silica based optical fibers), one laser frequency may act as a local oscillator for the detection of the Brillouin scattering spectrum. Optical heterodyning with the backscattered signal performs the detection at the lower frequency ($\Delta v - v_B$), where Δv is the difference between the two laser frequencies and v_B is the Brillouin frequency. Such a system has been proposed using two phase-locked fiber lasers [19]. Using a dual-frequency source in which the two frequencies share the same cavity may simplify the stabilization scheme. Based on this idea we are interested in the demonstration of a dual-frequency vertical external cavity surface emitting laser (VECSEL) emitting at 1.5 μm with a frequency difference close to the Brillouin frequency.

Before 2009, dual-frequency microchip lasers at 1.5 μm were based on diode-pumped solid-state gain medium (e.g. Yb:Er:Glass) [20]–[22]. A dual-frequency vertical-external-cavity-surface-emitting laser (VECSEL) emitting at 1 μm was first reported by Balli *et al.* [23] to benefit from the class A operation of this semiconductor disk laser, which is free from relaxation oscillations. The cavity concept was the same as for the dual-frequency glass-doped solid state lasers [22]. A Fabry-Perot (F-P) etalon was inserted in the extended cavity to select a single-longitudinal cavity mode, and a birefringent crystal (YVO_4 in the case of [22]) was used to ensure a frequency separation between the two orthogonal polarizations. In this first report, the VECSEL chip was grown on a GaAs substrate. The bottom, highly-reflective distributed Bragg reflector (DBR) consisted of alternating GaAs and AlGaAs quarter-wavelength layers and the active region consisted of InGaAs/GaAs quantum wells to emit around 1 μm. In 2012, Camargo *et al.* demonstrated the first dual-frequency VECSEL operating at 852 nm dedicated to the coherent population trapping of Cesium atoms [24]. The cavity principle was the same (a birefringent crystal and a F-P etalon were used), but this time the VECSEL active region was composed of GaAs quantum wells, embedded in AlGaAs barriers and pump-absorbing layers. The first dual-frequency VECSEL emitting at 1550 nm was reported in 2014 by De *et al.* [25], with the same cavity configuration. The VECSEL chip used InGaAlAs multi quantum-wells, grown on an InP substrate as the active region. Our aim is to realize a dual-frequency VECSEL emitting at 1550 nm with a frequency difference close to the scattered Brillouin frequency in standard single-mode fibers around 11 GHz. The realization of the 1.5 μm dual-frequency VECSEL source is detailed in the following. The achieved results are compared to the targeted specifications for a possible integration of the source in an OFS based on Brillouin scattering.

2. Experimental conditions

2.1. VECSEL chip fabrication

The VECSEL structure has been optimized to achieve a low lasing threshold, and high output power under optical pumping [26], [27]. The active region is grown on an InP substrate. It is designed for optical pumping at 980 nm and includes strained InGaAlAs quantum wells. A 17-pair $GaAs/Al_{0.97}Ga_{0.03}$ As semiconductor DBR is integrated to the active region using a metamorphic regrowth [26]. A gold layer is deposited on the surface of the Bragg mirror to enhance its reflectivity. The semiconductor chip with deposited gold is then integrated to a chemical vapor deposition (CVD) diamond host substrate using metallic bonding. The InP substrate, and the etch-stop layer are then removed using selective chemical etching. Finally, the InP top layer of the VECSEL is finely etched to tune the resonance wavelength of the microcavity close to 1550 nm. An anti-reflective (AR) coating at 980 nm is deposited on the surface to enhance pump absorption [28]. The completed VECSEL structure is schematically depicted in Fig. 1.

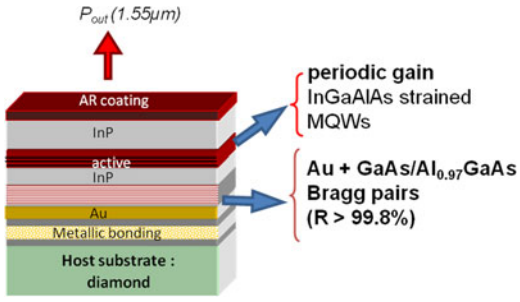

Fig. 1. VECSEL chip emitting at 1550 nm.

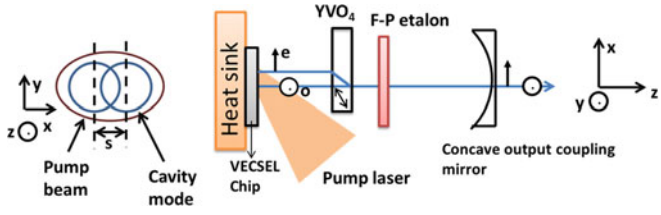

Fig. 2. Schematic of the dual-frequency VECSEL cavity. (Left) Schematics of the spatially separated cross-polarized cavity modes (blue) and pump spot (brown).

2.2. VECSEL cavity configuration

The dual-frequency laser cavity is schematically depicted in Fig. 2. The VECSEL chip is assembled with a highly reflective output coupling mirror to form a stable plane-concave cavity. The concave mirror used has a radius of curvature (R_{OC}) of 10 mm and a nominal reflectivity of 99.7%. A high reflectivity has been chosen to compensate for the optical losses potentially introduced by the intra-cavity elements. The VECSEL chip is fixed to a temperature-regulated copper plate. The operating temperature is set to 20 °C.

To achieve dual-frequency laser operation a birefringent crystal plate (YVO_4) cut at 45° of the crystal optical axis is inserted in the extended cavity. The plate is AR-coated at 1550 nm on both faces. This type of birefringent crystal leads to both a frequency separation and a spatial separation (s) of the two orthogonally-polarized longitudinal cavity modes. For a plate thickness of 500 μm, $s = 50\,\mu$m. An intra-cavity F-P etalon allows the selection of one longitudinal mode for each of the two polarizations. In our experiment a glass (SiO_2) etalon with a thickness of 160 μm (etalon free spectral range FSR = 5 nm at 1550 nm) is used. In order to achieve dual-frequency emission with a frequency difference close to 11 GHz, the cavity length was fixed to $L_{cav} \sim 9$ mm, corresponding to a FSR larger than 11 GHz. This should favor the selection of only one longitudinal mode for each of the two polarizations in the cavity FSR. With $R_{OC} = 10$ mm and $L_{cav} = 9$ mm the cavity mode radius is estimated to be $\omega_0 \sim 40\,\mu$m.

The VECSEL chip is pumped at 45° incidence using a single transverse mode laser diode emitting at 980 nm and having a maximum pump power of 1.3 W. The pump spot size ω_p can be adapted in the range of 40 to 90 μm in order to pump uniformly the two cavity modes separated by a distance s.

2.3. Characterization set-up

The characterization set-up is depicted in Fig. 3. A movable mirror is used to allow the measurement of the laser output power versus incident power (L-P curve).

For the purpose of beat-note characterization, an optical polarizer with a 45° orientation is used to combine the two orthogonal polarizations. The laser light is then injected in a fibered 1 × 2 coupler via an optical isolator. The first arm of the coupler is connected to the optical spectrum analyser

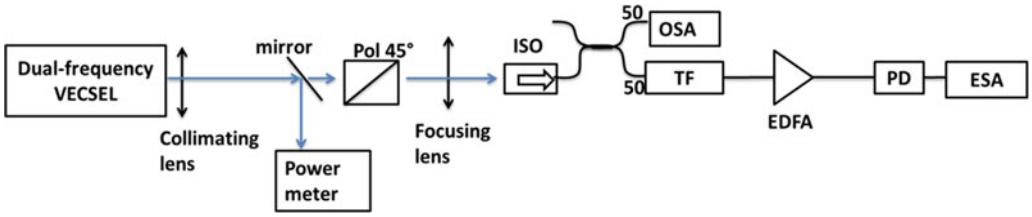

Fig. 3. Experimental set-up used for the measurements (Pol: Polarizer; ISO: Optical isolator; TF: Tunable optical filter (FWHM ~ 1.5 nm); OSA: Optical Spectrum Analyzer; EDFA: Erbium Doped Fiber Amplifier; PD: photodiode; ESA: Electrical Spectrum Analyser).

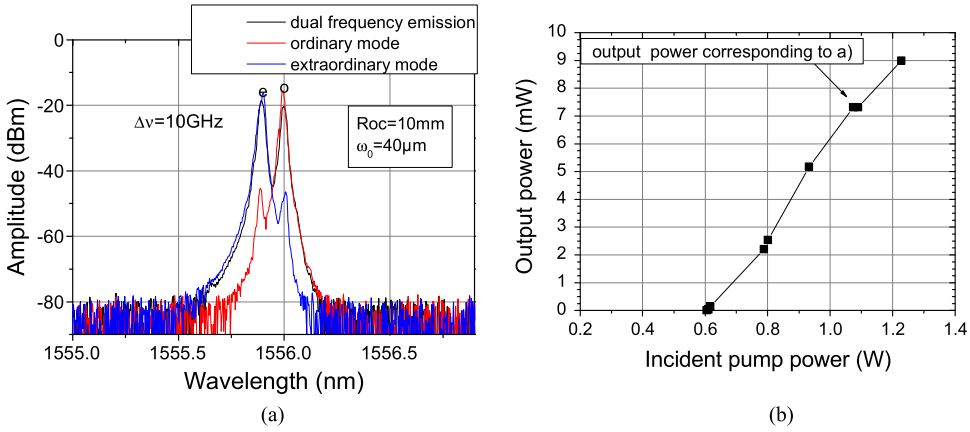

Fig. 4. (a) Optical spectrum of the dual frequency laser emission measured with the polarizer at 45° (black curve), at 90° (ordinary mode, red curve), and at 0° (extraordinary mode, blue curve). (b) Corresponding L-P curve. The other cavity parameters are $L_{cav} \sim 8.8$ mm, YVO_4 plate (500 μm thick), and SiO_2 F-P etalon (160 μm thick).

(OSA) while the second one is connected to an electrical spectrum analyser (ESA) for simultaneous measurement of both spectra. The spectral resolution of the OSA [resolution bandwidth (RBW)] is limited to 10 pm (~1.2 GHz). In a real OFS unit, the optical loss induced by the polarization combination for heterodyning could be compensated by using an optical/electrical pre-amplification stage and by increasing the incident power in the fiber.

Fig. 4(a) shows a typical optical spectrum obtained in dual-frequency operation using the intra-cavity elements mentioned in Section 2.2. The frequency measured difference (Δv) is 10 GHz close to the Brillouin scattering frequency. Fig. 4(b) shows the corresponding L-P curve in dual-frequency operation.

3. Results

3.1. Influence of the intra-cavity elements and output coupling mirror on the output power

Spontaneous Brillouin scattering takes place at low power levels, typically few milliwatts, but OFS based on stimulated Brillouin scattering require several tens of mW of optical power in the optical fiber. We have therefore evaluated the influence of the intra-cavity elements on the VECSEL efficiency and maximum output power. The L-P curve was first measured with no intra cavity elements in Fig. 5(a) and then with either the F-P etalon Fig. 5(c) or the YVO_4 plate inserted in the cavity Fig. 5(b).

It can be observed from Fig. 4(b) and Fig. 5(a) that the VECSEL output power is typically decreased by more than half in the dual-frequency case. The L-P curves measured with YVO_4

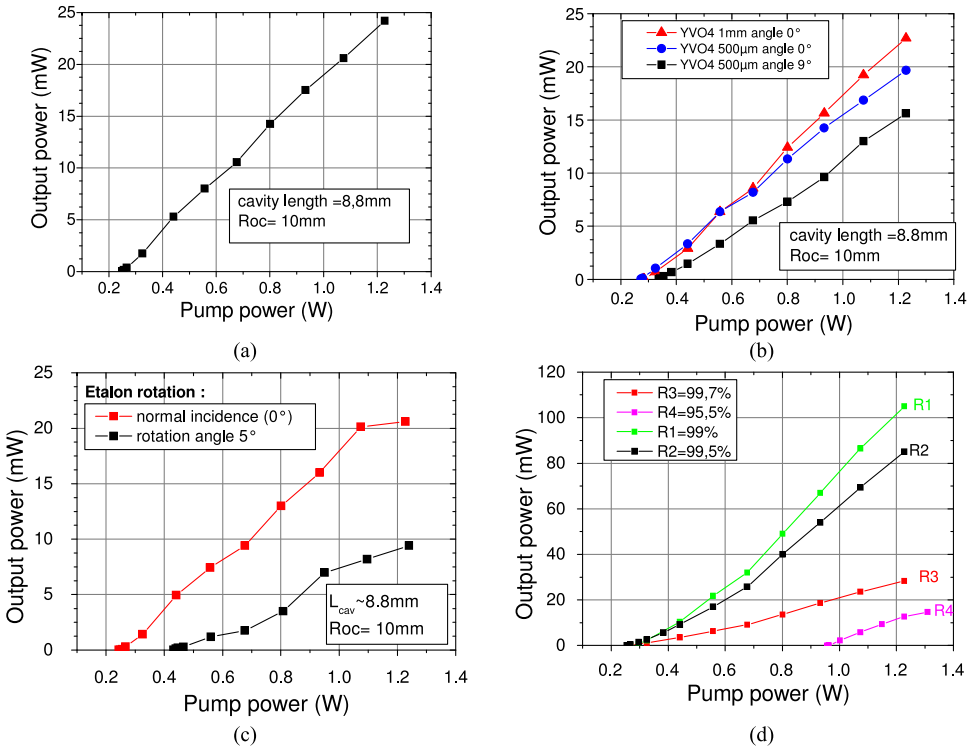

Fig. 5. L-P curve measured using the output coupler having a nominal reflectivity R = 99.7% without intra-cavity elements (a), with the 500 μm thick YVO_4 plate only inserted in the cavity (b), with the F-P etalon (SiO_2 plate) only inserted in the cavity (c), and without intra-cavity elements but with output couplers with different reflectivity values (d). The cavity length is fixed to L_{cav} = 8.8 mm in (a)–(c).

plates of different thicknesses and different orientations in the cavity are reported in Fig. 5(b). A 0° incidence means that the plate is normal to the cavity axis. The results of Fig. 5(b) show that neither the thickness of the birefringent crystal nor its rotation (by up to 9°) have a significant impact on the output power, indicating that the YVO_4 plate does not represent the main source of optical loss. Fig. 5(c) illustrates the influence of the rotation of the SiO_2 F-P etalon in the VECSEL cavity. The etalon is rotated in the same way as the YVO4 plate. A slight rotation of the etalon causes high intra-cavity losses and therefore a significant decrease of the VECSEL efficiency. This is the main origin of the limited output power in Fig. 4(b). It is, therefore, practically important to search for an "ideal" etalon allowing to achieve single longitudinal laser emission at 1.5 μm with an orientation close to 0°.

Finally the influence of the reflectivity of the output coupler on the VECSEL output power has also been investigated. For the comparison, no intra-cavity element has been used, and the cavity mode radius and the pump spot size are the same as in the previous experiments ($\omega_0 \sim$ 40 μm, and $\omega_P \sim$ 87 μm, respectively). The results are reported in Fig. 5(d). Using an output coupler reflectivity close to 99% increases the output power by a factor of 4, and up to 100 mW output power can be obtained in a simple cavity. The slight power difference between Fig. 5(d) with mirror R3, and Fig. 5(a) comes from the fact that a second cavity set-up has been used to compare the different output coupling mirrors. Since the VECSEL chip has been moved from one set-up to the other, the exact positioning of the pump spot on the VECSEL surface may be different in the experiments corresponding to Fig. 5(a)-(c) and to Fig. 5(d), which explains that the slight output power variation.

Mirror R1 could not be used in the dual-frequency set-up because of its too large external diameter leading to a partial screening of the pump beam. Provided that a mirror with the adapted dimensions is available, and taking into account the additional losses introduced by the F-P etalon, more than

50 mW output power may be expected in dual-frequency laser operation by using an output coupler having a reflectivity close to R1 $\sim$ 99%.This value may be compatible with both spontaneous and stimulated Brillouin scattering.

3.2. Influence of the birefringent crystal on the stability of the laser emission

Simultaneous oscillation of the cross-polarized cavity modes depends on the non-linear coupling constant (also referred to as the non-linear coupling strength) C between these modes [29]. The nonlinear coupling constant is related to the spatial overlap between the two modes r. r is written as

$$r = \frac{2\omega_0^2 \cos^{-1}\left(\frac{s}{2\omega_0}\right) - \frac{1}{2}\sqrt{\left(4s^2\omega_0^2 - s^4\right)}}{\pi\omega_0^2}$$

C is close to one if the spatial separation s between the two modes is null, due to the homogeneous gain of the VECSEL active region [30]. A coupling strength too close to 1 will induce mode competition and unstable dual-frequency operation [30]. On the other hand, widely spatially separated modes (i.e., with a coupling strength near zero) may present uncorrelated noise and, therefore, a broader and less stable beat note. For intermediate values of C, it has been shown that the phase noise of the RF beat-note due to pump intensity fluctuations transferred to the intensity noises of the two lasing modes and to the phase noise via the Henry factor of the semiconductor gain medium depends on the coupling strength [31].

We have examined the influence of r (and, hence, of the nonlinear coupling strength between the two eigenstates in the active medium) on the stability of the dual-frequency laser emission. In order to vary r, we have either changed the thickness of the birefringent crystal or the size of the cavity mode. Four different cases with different r coefficients have been compared. The first case, with $r = 0$ has been obtained with an YVO_4 plate having a thickness of 1 mm (corresponding to s = 100 μm), and a mode radius $\omega_0 = 40$ μm. The second case, with $r = 25\%$ is obtained in the same conditions but with a 500 μm thick YVO_4 plate (s = 50 μm). To increase r to 50% the output coupler is replaced by a second one having the same reflectivity and a radius of curvature $R_{OC} = 12$ mm, leading to a cavity mode radius $\omega_0 = 50$ μm, the other cavity conditions being the same as in the second case. Finally $r = 70\%$ has been was obtained using $R_{OC} = 10$ mm, and a 250-μm thick YVO_4 plate (s = 25 μm). In all cases a 160 μm thick F-P etalon is used, and the cavity length is fixed to $L_{cav} \sim 8.8$ mm.

The stability of the dual-frequency emission has been assessed by recording the optical spectrum over several minutes. The optical spectra are reported in Fig. 6(a)-(d). It can be observed that dual-frequency laser emission with a stable intensity per mode and stable frequency difference can be obtained for $r = 0\%$ to 70% with our VECSEL structure. The variation of the frequency difference versus time is reported in Fig. 7. The measurement is mainly limited by the OSA resolution bandwidth, but it can be concluded that the long-term temporal drift of the frequency difference is lower than 1 GHz over 10 min in free-running conditions.

3.3. Influence of the Fabry-Perot etalon on the stability of the laser emission

As mentioned in Section 2, it is important to maintain single-longitudinal lasing on each of the two polarizations in order to obtain a stable dual-frequency laser emission. The FSR of the intra-cavity F-P etalon must be large enough to avoid simultaneous lasing of cavity modes located at different successive transmission maxima of the etalon. For this reason, using the same cavity elements as in Fig. 4, we have replaced the 160 μm thick SiO_2 etalon (FSR = 5 nm) by another one (SiO_2, thickness of 50 μm and FSR = 13 nm). The F-P etalon is placed in the cavity close to normal incidence. Using a F-P etalon having a large FSR ($\sim$13 nm), it is easier to select one longitudinal cavity mode located close to only one transmission maximum of the etalon. However, in this case, a dual-frequency emission with frequencies largely separated (up to 30 GHz) is generally obtained,

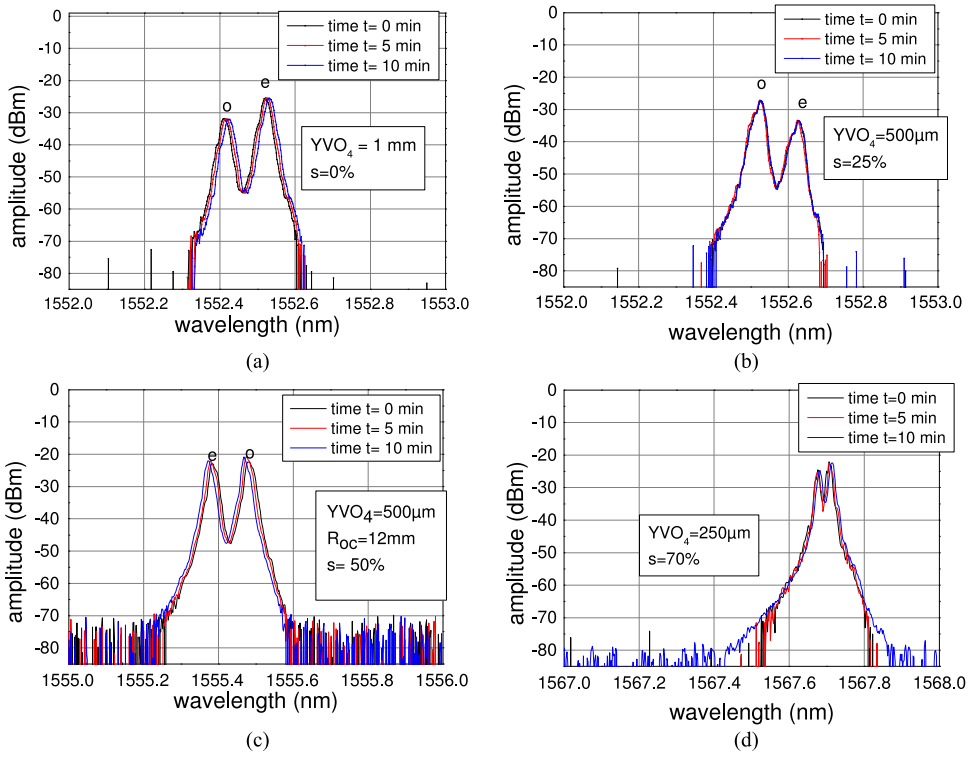

Fig. 6. Optical spectrum of the dual-frequency laser emission recorded with the OSA over several minutes with r = 0% (a), r = 25% (b), r = 50% (c), and r = 70% (d). The OSA resolution bandwidth is fixed to RBW = 0.01 nm.

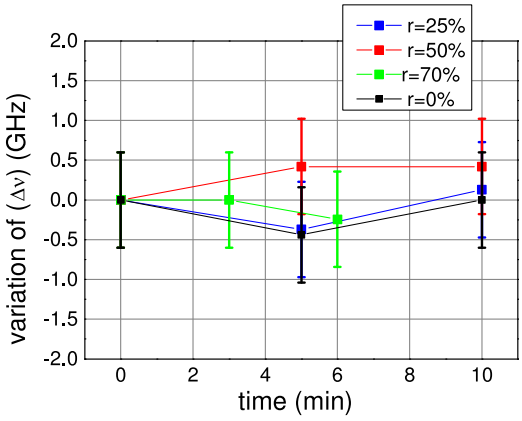

Fig. 7. Variation of the frequency difference $\Delta\nu$ versus time for different *r* coefficients as deduced from the optical spectra of Fig. 6.

and the frequency difference is not stable, as illustrated in Fig. 8. A frequency difference close to 11 GHz or lower is systematically obtained with the thicker etalon.

The cavity mode radius and the YVO_4 plate thickness being the same in the two experiments, it can be considered that the coupling strength between the modes is similar, and we speculate that the observed behavior can be attributed to an etalon effect. The bandwidth of the thinner etalon is indeed also larger allowing to select two orthogonal modes with a larger frequency separation, which may present less mode competition due to weaker coupling.

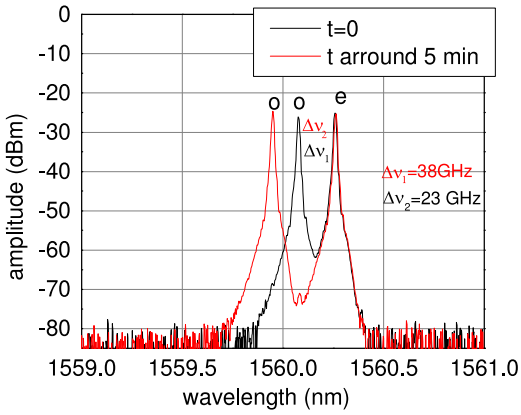

Fig. 8. Evolution with time of the optical spectrum of the dual-frequency laser emission obtained with a 50 μm thick SiO_2 F-P etalon. The other cavity parameters are the same as in Fig. 4.

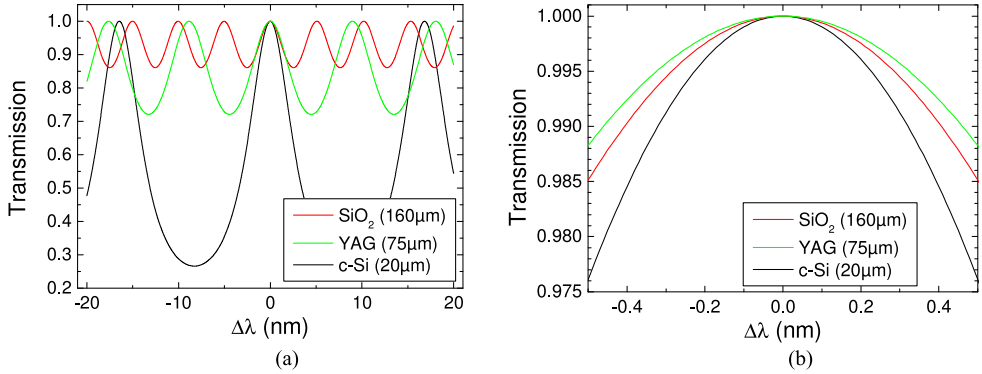

Fig. 9. Comparison between the transmission functions of three etalons having different thickness and refractive indices at 1.5 μm (red curve: 160 μm thick SiO_2 etalon, green curve: 75 μm thick YAG etalon, black curve: 20 μm thick Si etalon). (a) Large view of the transmission function showing the FSR. (b) Closer view showing the etalon bandwidth at T $=$ 99%.

It can be concluded that an ideal F-P etalon would have a FSR close to that of the 50 μm thick SiO_2 etalon (FSR $\sim$ 13 nm) and a bandwidth close to that of the 160 μm thick SiO_2 etalon to ensure stable dual frequency laser emission. This may be achieved by using a YAG or Si etalon with the adapted thickness, as illustrated in Fig. 9.

3.4. Influence of the mechanical vibrations on the stability without active stabilization

Finally, we have examined the stability of the beat-note frequency in the MHz range using the experimental set-up shown in Fig. 3.

A typical electrical spectrum corresponding to a frequency difference of 9.85 GHz is shown in Fig. 10. The full width at half-maximum (FWHM) can be estimated to be of the order of 200 kHz. Dual-frequency VECSELs operating at 850 nm and using a similar cavity configuration have shown a beat note width of 150 KHz with no active stabilization [24], which is similar to the above result. In order to estimate the temporal jitter and drift of the frequency difference, the signal has also been acquired with a resolution bandwidth of 1 kHz and a sweep time of 50 s to 75 s. From the envelop of the signal, an overall drift of $\sim$1 MHz per minute can be estimated. We attribute this relatively large drift under free-running conditions to mechanical instabilities in our experimental setup.

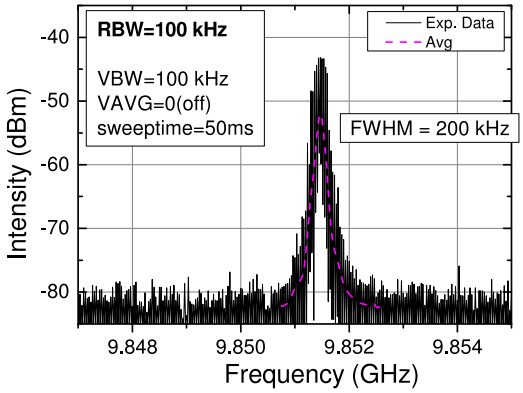

Fig. 10. Electrical spectrum recorded with the electrical spectrum analyzer (ESA) for a cavity length of ∼8.8 mm and an YVO_4 plate thickness of 500 μm. The ESA resolution bandwidth (RBW) and video bandwidth (VBW) were set to 100 kHz. No video averaging (VAVG) of the trace was used.

A beat note linewidth and a temporal jitter and drift of the frequency difference typically lower than 0.5 MHz over 10 minutes (the typical duration of one acquisition) would be necessary to allow the detection of 0.5 °C temperature variation in the single mode fiber (SMF) with an OFS based on Brillouin scattering [32].

4. Conclusion

We have fabricated a VECSEL chip for laser emission at 1.5 μm, and we have assembled a VECSEL cavity for dual-frequency operation in this wavelength window. Our objective is to produce a stable beat note close to the Brillouin frequency. The experimental results show that an output power up to 50 mW can be expected in dual-frequency operation, which is compatible with both a spontaneous and stimulated Brillouin scattering. A stable dual frequency emission has been demonstrated for mode spatial overlap from 0% to 70%. The optimization of the intra-cavity elements, mainly the F-P etalon can help to ensure a long-term stability of the dual-frequency emission without mode hoping. In the stability range explored in this work, the mode coupling strength has a second order influence on the stability of the dual-frequency emission, allowing to adapt the cavity mode size to the pump spot size to improve the laser efficiency. The beat-note linewidth is measured to be ∼240 kHz with a temporal drift of the order of 1 MHz/min for the free running laser. Presently, mechanical vibrations appear to be the main cause of the frequency difference instability. The design of a mono-block cavity may allow to meet the stability requirements for optical fiber Brillouin sensors.

References

[1] S. Yang and S. Zhang, "The frequency split phenomenon in a He-Ne laser with a rotational quartz," *Opt. Commun.*, vol. 68, no. 1, pp. 55–57, Sep. 1988.
[2] S. Zhang, M. Lu, G. Jin, and M. Wu, "Laser frequency split by an electro-optical element in its cavity," *Opt. Commun.*, vol. 96, nos. 4–6, pp. 245–248, Feb. 1993.
[3] Y. Han, Y. Zhang, Y. Li, and S. Zhang, "Two kinds of novel birefringent dual-frequency lasers," *Opt. Laser Eng.*, vol. 31, no. 3, pp. 207–212, Mar. 1999.
[4] T. Yoshino and Y. Kobayashi, "Temperature characteristics and stabilization of orthogonal polarization two-frequency Nd3+:YAG microchip lasers," *Appl. Opt.*, vol. 38, no. 15, pp. 3866–3270, May 1999.
[5] M. Brunel, F. Bretenaker, and A. Le Floch, "Tunable optical microwave source using spatially resolved laser eigenstates," *Opt. Lett.*, vol. 22, no. 6, pp. 384–386, Mar. 1997.
[6] J. Czarske and H. Muller, "Heterodyne interferometer using a novel two-frequency Nd:YAG laser," *Electron. Lett.*, vol. 30, no. 12, pp. 970–971, Jun. 1994.
[7] J. W. Czarske and H. Mueller, "Birefringent Nd:YAG microchip laser used in heterodyne vibrometry," *Opt. Commun.*, vol. 114, nos. 3–4, pp. 223–229, Feb. 1995.

[8] S. Zhang, K. Li, M. Ren, and Z. Deng, "Investigation of high-resolution angle sensing with laser mode-split technology," *Appl. Opt.*, vol. 34, no. 12, pp. 1967–1970, Apr. 1995.
[9] A. J. Seeds, "Microwave photonics," *IEEE Trans. Microw. Theory Techn.*, vol. 50, no. 3, pp. 877–887, Mar. 2002.
[10] J. Yao, "Microwave photonics," *J. Light. Technol.*, vol. 27, no. 3 pp. 314–335, Feb. 2009.
[11] D. Wake, C. Lima, and P. A. Davies, "Optical generation of millimeter- wave signals for fiber-radio systems using a dual-mode DFB semiconductor laser," *IEEE Trans. Microw. Theory Techn.*, vol. 43, no. 9, pp. 2270–2276, Sep. 1995.
[12] X. Chen, Z. Deng, and J. Yao, "Photonic generation of microwave signal using a dual-wavelength single-longitudinal-mode fiber ring laser," *IEEE Trans. Microw. Theory Techn.*, vol. 54, no. 2, pp. 804–809, Feb. 2006.
[13] J. O'Reilly and P. Lane, "Fibre-supported optical generation and delivery of 60 GHz signals," *J. Lightw. Technol.*, vol. 12, no. 16, pp. 1329–1330, Aug. 1994.
[14] A. Kaszubowska, P. Anandarajah, and L. P. Barry, "Improved performance of a hybrid radio/fibersystem using a directly modulated lasertransmitter with external injection," *IEEE Photon. Technol. Lett.*, vol. 14, no. 2, pp. 233–235, Feb. 2002.
[15] F. Friederich, G. Schuricht, and A. Deninger, "Phase-locking of the beat signal of two distributed-feedback diode lasers to oscillators working in the MHz to THz range," *Opt. Exp.*, vol. 18, no. 8, pp. 8621–8629, Apr. 2010.
[16] L. A. Johansson and A. J. Seeds, "Millimeter-wave modulated optical signal generation with high spectral purity and wide-locking bandwidth using a fiber-integrated optical injection phase-lock loop," *IEEE Photon. Technol. Lett.*, vol. 12, no. 6, pp. 690–692, Jun. 2000.
[17] R. C. Steele, "Optical phase-locked loop using semiconductor laser diodes," *IEEE Photon. Technol. Lett.*, vol. 19, no. 2, pp. 69–71, Jan. 1983.
[18] J. Geng, S. Staines, M. Blake, and S. Jiang, "Distributed fiber temperature and strain sensor using coherent radio-frequency detection of spontaneous Brillouin scattering," *Appl. Opt.*, vol. 46, no. 23, pp. 5928–5932, Aug. 2007.
[19] J. Geng, S. Staines, Z. Wang, J. Zong, M. Blake, and S. Jiang, "Highly stable low-noise brillouin fiber laser with ultranarrow spectral linewidth," *IEEE Photon. Technol. Lett.*, vol. 18, no. 17, pp. 1813–1815, Sep. 2006.
[20] M. Alouini, M. Brunel, F. Bretenaker, and M. Vallet, "Dual tunable wavelength Er,Yb:Glass laser for terahertz beat frequency generation," *IEEE Photon. Technol. Lett.*, vol. 10, no. 10, pp. 1554–1556, Nov. 1998.
[21] M. Brunel, A. Amon, and M. Vallet, "Dual-polarization microchip laser at 1.53 μm," *Opt. Lett.*, vol. 30, no. 18, pp. 2418–2420, Sep. 2005.
[22] G. Pillet *et al.*, "Dual-frequency laser at 1.5 μm for optical distribution and generation of high-purity microwave signals," *J. Lightw. Technol.*, vol. 26, no. 15, pp. 2764–2773, Aug. 2008.
[23] G. Baili *et al.*, "Experimental demonstration of a tunable dual-frequency semiconductor laser free of relaxation oscillations," *Opt. Lett.*, vol. 34, no. 21, pp. 3421–3423, Nov. 2009.
[24] F. A. Camargo *et al.*, "Coherent dual-frequency emission of a vertical external-cavity semiconductor laser at the cesium D2 line," *IEEE Photon. Technol. Lett.*, vol. 24, no. 14, pp. 1218–1220, Jul. 2012.
[25] S. De, G. Baili, M. Alouini, J.-C. Harmand, S. Bouchoule, and F. Bretenaker, "Class-A dual-frequency VECSEL at telecom wavelength," *Opt. Lett.*, vol. 39, no. 19, pp. 5586–5589, Oct. 2014.
[26] J-P. Tourrenc *et al.*, "Thermal optimization of 1.55 um OP-VECSEL with hybrid metal-metamorphic mirror for single-mode high power operation," *Opt. Quantum Electron.*, vol. 40, no. 2, pp. 155–165, Mar. 2008.
[27] S. Bouchoule *et al.*, "Picosecond to sub-picosecond pulse generation from mode-locked VECSELs at 1.55 μm," *Proc. SPIE*, vol. 8242, Jan. 21–26, 2012, Art. no. 824203.
[28] Z. Zhao *et al.*, "Cost-effective thermally-managed 1.55 μm VECSEL with hybrid mirror on copper substrate," *IEEE J. Quantum Electron.*, vol. 48, no. 5, pp. 643–650, May 2012.
[29] M. Alouini, F. Bretenaker, M. Brunel, A. Le Floch, and M. Vallet, "Existence of two coupling constants in microchip lasers," *Opt. Lett.*, vol. 25, no. 12, pp. 896–898, Jun. 2000.
[30] V. Pal *et al.*, "Measurement of the coupling constant in a two-frequency VECSEL," *Opt. Exp.*, vol. 18, no. 5, pp. 5008–5014, Mar. 2010.
[31] S. De *et al.*, "Phase noise of the radio frequency (RF) beatnote generated by a dual-frequency VECSEL," *J. Lightw. Technol.*, vol. 32, no. 7, pp. 1307–1316, Apr. 2014.
[32] K. Shimizu, T. Horiguchi, Y. Koyamada, and T. Kurashima, "Coherent self-heterodyne detection of spontaneously Brillouin-scattered light waves in a single-mode fiber," *Opt. Lett.*, vol. 18, no. 3, pp. 185–187, Feb. 1993.